Archives of Food Science and Technology

Research Article
Published: 20 Jan, 2020

Effective Adsorption and Separation of Lysozyme with Magnetite/Isinglass Composite Nanoparticles: Investigation of the Operational Parameters

Afsaneh Mollahosseini[1], Farid Mostafaei[1], Ali Khadir[2], Shahrzad Javanshir[1] and Elham Pourian[1]*

[1]*Department of Chemistry, Iran University of Science and Technology, Iran*

[2]*Department of Civil and Environmental Engineering, Iran University of Science and Technology, Iran*

Abstract

The present study focused on the separation of lysozyme from various media using adsorption technology. Firstly, Fe_3O_4/isinglass nanocomposite was synthesized and then characterized by Fourier Transform Infrared Spectrometer (FTIR), Scanning Electron Microscope (SEM), Transmission Electron Microscopy (TEM) and Vibrating Sample Magnetometer (VSM). The maximum adsorbent capacity was achieved at a contact time of 90 min, pH of 6.2, the initial LYZ concentration of 0.5 mg ml^{-1}, and the adsorbent dosage of 15 mg. The obtained experimental data suited well with the Langmuir isotherm model by prediction the maximum adsorption capacity and a correlation coefficient of 149.25 mg/g and 0.9532, respectively. The kinetic data were well fitted using a pseudo second order kinetic model. Under optimized condition, the relative standard deviation with three replicates was 3.2%. The mixture of lysozyme and bovine serum albumin was used as a mixture model protein to investigate the adsorption selectivity. The magnetite/isinglass composite was then used for the extraction of lysozyme from egg white solutions. Sodium Dodecyl Sulfate-Polyacrylamide Gel Electrophoresis (SDS-PAGE) results showed that adsorption of lysozyme from protein mixture is selective and extracted lysozyme from egg white showed high purity.

Keywords: Protein separation; Lysozyme; Egg white; Fe_3O_4@IG nanoparticles; Adsorption

OPEN ACCESS

Correspondence:
Afsaneh Mollahosseini, Department of Chemistry, Research Laboratory of Spectrometry & Micro and Nano Extraction, Iran University of Science and Technology, Tehran, Iran, Tel: +98 21 77240540; Fax: +98 21 73021578; E-mail: amollahosseini@iust.ac.ir

Received Date: *25 Oct 2019*
Accepted Date: *02 Jan 2020*
Published Date: *20 Jan 2020*

Citation:
Mollahosseini A, Mostafaei F, Khadir A, Javanshir S, Pourian E. Effective Adsorption and Separation of Lysozyme with Magnetite/Isinglass Composite Nanoparticles: Investigation of the Operational Parameters. Arch Food Sci Technol. 2020; 1(1): 1003.

Introduction

Lysozyme (LYZ), also called muramidase or N-acetyl muramic hydrolase, is a low molecular weight protein accidentally discovered by Alexander Fleming in 1922 [1]. LYZ is widely available in human organs, tissues, and secretions and can be categorized into three distinct groups namely, chicken type (c-type), goose type (g-type) and invertebrate-type (i-type). Of these, c-type obtained vastly from hen egg white, has gained much attention because of its unique characteristics and abundance [2]. Many studied have found that LYZ has a great antibacterial activity toward wide groups of Gram-positive bacteria and modification of LYZ with heat, chemicals, and hydrolysis can broaden its application [3]. So, LYZ is used as a natural food preservative for meat, dairy products, and fish industry. FAO/WHO Food Standards allowed the use of LYZ in cider and perry manufacture, grape wines and ripened cheeses [4]. Surprisingly, LYZ has exhibited capability in pharmaceutical used and been used as anticancer drugs and HIV treatment [5-7]. Based on the above advantages, separation and purification of LYZ through facile and easily scale-up technologies has been attracted great attention. In this direction, various methods have been reported to separate lysozyme from aqueous media. Wan et al. [8] studied the separation of lysozyme from natural chicken egg white with through ultra filtration method and reported that more than 94% of lysozyme was observed in the permeate. Chen et al. [9] utilized a combination of reductants and thermal treatment to recover lysozyme from egg whites. Nom and Imm extracted lysozyme from reconstituted freeze-dried egg-white by using the reverse micelles and under optimum conditions reached 96% of lysozyme recovery [10]. Other methods to separate LYZ such as precipitation [11], nanofiltration [12], crystallization [13] and expanded and/or fluidized bed chromatography have been also investigated and exhibited high efficiency, however, most of these methods are expensive, hard operation, and of course, time consuming [14]. To solve the mentioned problems, adsorption was proposed. Adsorption, physical separation through the transportation of the protein molecules from the bulk solution to a solid

surface called adsorbent, has gained much attention recently in the various field of separation and purification technology because of its easy operation, high efficiency and cheap to some degree [15]. pH, temperature, contact time, the presence of other competing ions and ionic strength of the solution are main parameters affecting adsorption efficiency but there is no any doubt that nature of the adsorbent is highly important that indirectly influences other parameters. In the case of LYZ separation, various adsorbent has been employed including acrylic acid copolymer based beads (Hydrolite D115), hybrid Zwitterionomer, monolithic molecularly imprinted cryogel, Carbon coated Fe_3O_4 nanoparticles, Sulfonated poly (glycidyl methacrylate) grafted cellulose, Tris(hydroxymethyl)aminomethane-modified magnetic microspheres. Apart from these materials, Isinglass (IG) has been recently introduced as a novel adsorbent. IG is derived from the swim bladder of certain fish and for many years has been utilized to clarify alcoholic beverages by aggregation of the yeast cells and other insoluble particles in the solution [16]. As a matter of fact, IG is somehow the waste of the fish industry and is abundantly available and can be easily found at low cost [17]. Surprisingly, the presence of the various functional groups such as OH, COHN, $-NH_2$, $-CONH_2$, and -COOH in IG, have nominated it as an effective adsorbent for adsorption process [18].

In every treatment technology, sludge will be generated in which collection and management of that is of great concern. Sedimentation tanks, filtration, and centrifugation are conventional methods to separate sludge involve advantages and disadvantages. Although sludge generated during the adsorption process is low, its collection from the solution body needs some considerations. Recently, the use of Fe_3O_4 within the adsorbent has resolved the issues. In fact, by employing an external magnetic field, the adsorbent can be easily gathered together. Furthermore, provision of the large surface area and better dispersion in water are another advantages of magnetic adsorbent which are beneficial for adsorption processes. In this work, the removal of LYZ from aqueous solution was investigated using Fe_3O_4 magnetite nanoparticles. The effects of the main parameters, i.e., contact time; pH, initial LYZ concentration, adsorbent dosage, and ionic strength were studied. The kinetic data were analyzed using pseudo first order and pseudo second order models and equilibrium data were fitted to two widely used isotherm models including Langmuir and Freundlich. Additionally, separation of LYZ from protein mixture and egg white solutions were studied.

Materials and Methods

LYZ, Bovine Serum Albumin (BSA), Glutaraldehyde (GA), ferric chloride hexahydrate ($FeCl_3.6H_2O$) and ferrous chloride tetrahydrate ($FeCl_2.4H_2O$) were purchased from Sigma-Aldrich Company (USA). Sodium hydroxide (NaOH), Potassium dihydrogen phosphate (KH_2PO_4), Sodium chloride (NaCl) and hydrochloric acid (HCl) were obtained from Merck Company (Darmstadt, Germany). The protein concentration was analyzed using UV/Vis Spectrometer (T80+ PG Instruments Ltd). The FTIR spectra of IG and Fe_3O_4@IG were conducted to specify the presence of functional groups on the synthesized adsorbents and it was done by Shimadzu FTIR spectrometer (Shimadzu, Japan). TEM images were carried out on EM10C-100 kV transmission electron microscope (Zeiss-Germany). The morphologies of the magnetic IG nanoparticles were observed using SEM, scanning electron microscope (EM-3200, KYKY, China). The magnetization characterization of Fe_3O_4 and Fe_3O_4@IG was performed on a vibrating sample magnetometer (Lake Shore 7410, USA).

Synthesis of Fe_3O_4 nanoparticles

The Fe_3O_4 Magnetite Nanoparticles (MN) through chemical co-precipitation method was synthesized by following the procedure. Firstly, iron solutions of 5.20 g $FeCl_3.4H_2O$ and 2.00 g $FeCl_2.4H_2O$ were dissolved in 25 ml N2 purged deionized water and the ratio of Fe2+ to Fe3+ was 2:1. A homogenous solution must be observed in this step. Under continuous stirring at 80°C for 60 min, slow addition of NaOH solution (1.50 mg/l) was done to adjust the pH value to 10 and consequently, chemical precipitation occurred. To separate precipitated products, an external magnetic field was employed. The obtained material was washed with deionized water and 25 ml ethanol for various times and then placed in an oven at 65°C for 24 h to become dry. The dried product is called Fe_3O_4 MN.

Preparation of IG

In order to prepare IG, fish bladders were first washed to remove any impurities and unwanted materials. Cut bladders were soaked in ethanol and stirred for 24 h. After stirring, the solution was filtered, washed with water, and placed in an open air for 24 h to become dry. To obtained IG fine powder, it was ground in a ball mill.

Preparation of Fe_3O_4@IG

0.1 g Fe_3O_4 and 10 ml GA in 15 ml of ethanol was stirred under reflux for 30 min. Then 0.1 g IG was added to the flask and the reaction was stirred for 1 h. After a specified time, heating was stopped and the reaction mixture was stirred for 30 min. After 2 h, the prepared magnetite IG by an external magnetic field was isolated and it was placed in an oven at 60°C to 70°C for 24 h.

Adsorption studies

Batch adsorption experiments were conducted in a 5 ml glass bottle, where the LYZ concentration, pH, and Fe_3O_4@IG dosage were fixed at 5 mg/ml, 6.4 mg and 20 mg, respectively. In the course of adsorption reaction, Fe_3O_4@IG loaded with LYZ was collected with the help of an external magnetic field and residue LYZ concentration was determined by use of a UV spectrophotometer at maximum absorbance (λ_{max}). In this direction, (λ_{max}) of LYZ was found to be 280 nm. The effects of contact time (0 min to 180 min); pH value (6.5 to 8.5), initial LYZ concentration (0 to 1.2 mg/ml), adsorbent dosage (0 mg to 25 mg), and ionic strength (0% to 20% w/v NaCl concentration) on the adsorption process were tested at a constant time 298 K and agitation speed of 160 rpm. The amount of LYZ adsorbed at equilibrium qe (mg/g) and the removal percentage were calculated by the following equations:

$$q_t = (C_o - C_t)\frac{V}{m}$$

$$\text{Removal rate (\%)} = \frac{C_o - C_t}{C_o}$$

Where C_o (mg/g) is the initial LYZ concentration, C_t (mg/g) is the concentration of LYZ at time t, V (L) is the volume of the solution, and m (g) is the mass of adsorbent used.

Desorption

Desorption of the adsorbed LYZ from Fe_3O_4@IG nanoparticles was studied in a batch experimental setup. LYZ adsorbed Fe_3O_4@IG nanoparticles (20 mg approximately) were placed in a phosphate buffer solution containing 10% w/v NaCl at pH=6 and shaken continuously at room temperature for 2 h. The final LYZ concentration in the desorption medium was determined spectrophotometrically at 280 nm. The desorption efficiency was calculated based on the amount

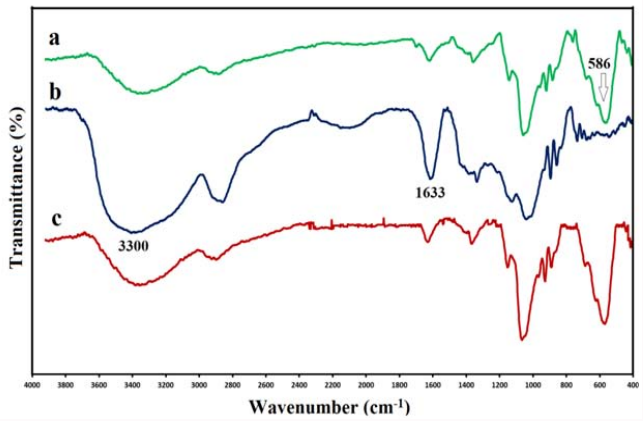

Figure 1: a) FTIR spectra of Fe_3O_4, b) IG, c) Fe_3O_4@IG.

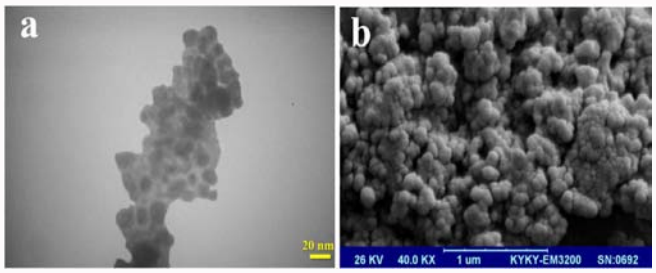

Figure 2: a) TEM, b) SEM images of Fe_3O_4@IG.

of LYZ in eluent and the adsorbed amount of lysozyme by Fe_3O_4@IG nanoparticles.

Separation of LYZ from binary protein mixture

20 mg Fe_3O_4@IG nanoparticles were added to a binary protein mixture of LYZ and BSA, the ratio of LYZ to BSA was 1:1 and the concentration of LYZ and BSA in the mixture was 0.5 mg ml^{-1}. The adsorption experiments were carried out in a protein mixture solution at 25°C for 90 min incubation and pH 7.4. Then protein laden magnetic adsorbent was separated with a magnet and desorbed in a phosphate buffer solution with pH 6 containing 10% w/v NaCl. The desorbed protein solution, the supernatant, and the stock binary protein solution were examined using Sodium Dodecyl Sulfate-Polyacrylamide Gel Electrophoresis (SDS-PAGE) with 12% separating gel, 5% stacking gels and stained with brilliant blue R250, according to the different molecular weights of a standard mixture of proteins.

Lysozyme extraction from egg white solutions

Chicken egg white was collected from fresh eggs and was diluted to 2% (v/v) with phosphate buffer (pH 7.4). The diluted solution was centrifuged at 4°C at 14,000 rpm for 60 min. The supernatant was used as the source chicken egg white solution for the extraction of LYZ. Then, 20 mg of dry Fe_3O_4@IG was added into 4 ml of Chicken egg white diluted solution and shaken at 298 K by vortex for 90 min. Then, Fe_3O_4@IG loaded with LYZ was collected from the solutions by a magnet. Finally, the components of proteins in the source chicken egg white solution, the supernatant after adsorption, and the eluted solution were examined using Sodium Dodecyl Sulfate-Polyacrylamide Gel Electrophoresis (SDS-PAGE) according to the previous section.

Results and Discussion

Characterization of the Fe_3O_4@IG

FTIR test: FTIR test was used to analyze the presence of functional groups in the synthesized adsorbent. Figure 1a shows the FTIR of Fe_3O_4 and it can be observed that there is a peak at 586 cm^{-1} which could be attributed to the (Fe-O) stretching vibration. In the FTIR spectra of IG (Figure 1b), peaks at 1633, and 586 cm^{-1} correspond to the presence of -NH_2 groups and the OH stretching vibration, respectively. Figure 1c presents the FTIR of the Fe_3O_4@IG that it is clearly evident that Fe_3O_4 was well coated with IG (Figure 1).

SEM and TEM images: Surface morphology of an adsorbent directly affects the adsorption process and so TEM and SEM images of the synthesized adsorbent were taken (Figure 2). It is obviously clear from the figure that Fe_3O_4@IG nanoparticles are spherical in shape with numerous sites for LYZ molecules to be adsorbed. According to the TEM image, Fe_3O_4@IG nanoparticles have a diameter of approximately 20 nm. Furthermore, IG acted like a surrounding shell (gray in color) around Fe_3O_4 (dark in color). It showed that IG was coated on the external surface of the Fe_3O_4 and Fe_3O_4 was like a core (Figure 2).

Magnetic properties of Fe_3O_4 and Fe_3O_4@IG: Magnetization curves of Fe_3O_4 and Fe_3O_4@IG at 300K were measured by VSM methods and the obtained data are illustrated in Figure 3. The figure indicated that the saturation magnetization of the Fe_3O_4 and Fe_3O_4@IG were 53.2 and 23.3 emu g^{-1}, respectively. The presence of the IG in the synthesized adsorbent could be confirmed by the fact that the saturation magnetization of the synthesized adsorbent decreased once Fe_3O_4 was coated with IG. Based on the previous reports, a saturation magnetization value greater than 16.3 emu g^{-1} is sufficient to separate adsorbent from the aqueous solution. Thus, in the present study, an external magnetic field was employed to separate Fe_3O_4@IG from the solution (Figure 3).

The effect of contact time

The effect of contact time on LYZ adsorption by Fe_3O_4@IG was determined using a 5 ml solution with 0.5 mg ml^{-1} LYZ at an adsorbent dosage of 20 mg, pH 6.4 and room temperature. The adsorption capacity was calculated at contact times ranging from 0 min to 180 min and the obtained results are illustrated in Figure 4a. It is evident from the figure that at the initial step of adsorption process (approximately 30 min), adsorption capacity exhibited a significant rapid increase, and however, a further increase in

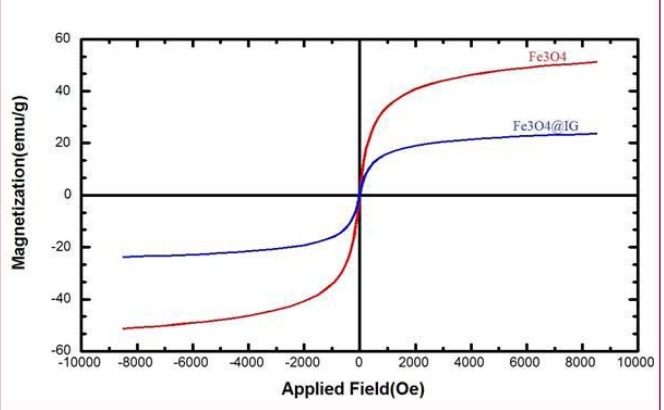

Figure 3: VSM spectra of Fe_3O_4 and Fe_3O_4@IG.

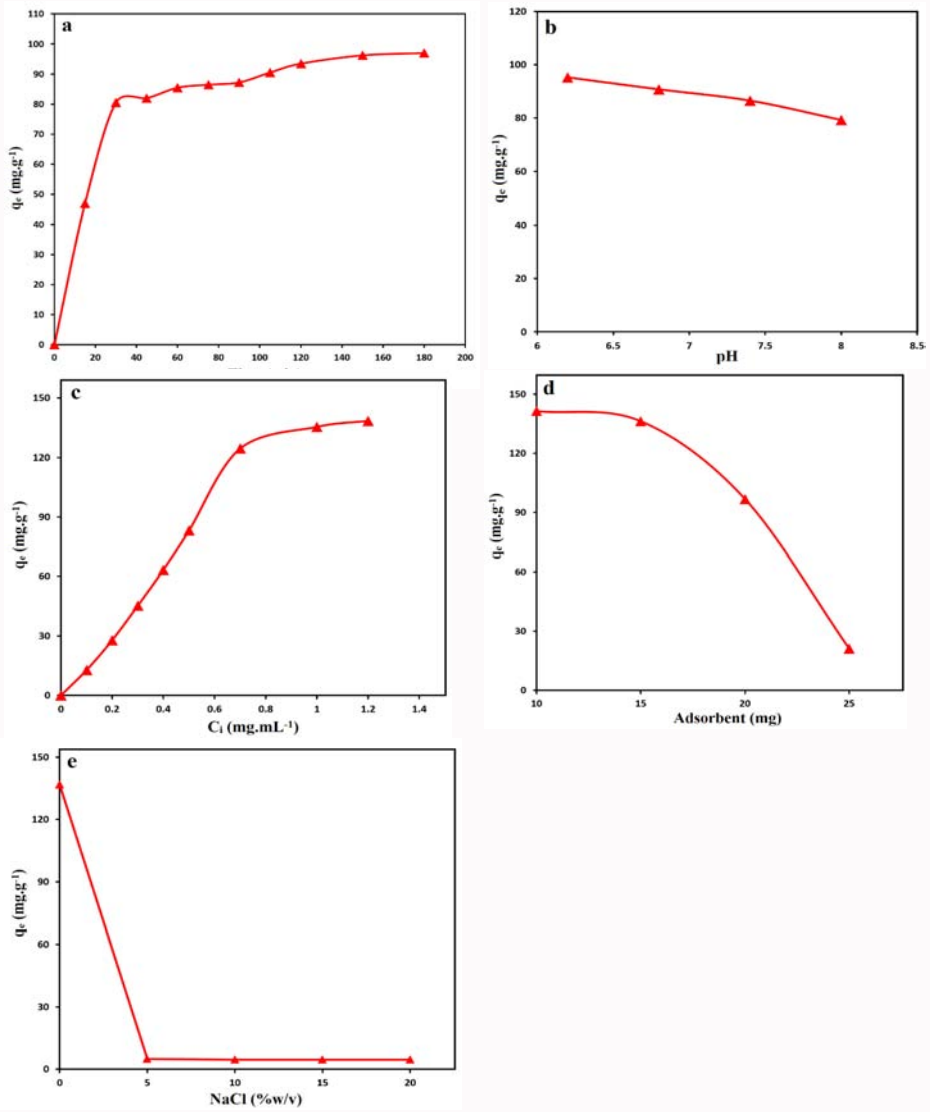

Figure 4: a) Effect of contact time to the adsorbing process (initial concentration of lysozyme: 0.5 mg ml^{-1}; pH: 6.4; temperature: 25ºC; adsorbent dosage: 20 mg, b) pH to the adsorbing process (initial concentration of lysozyme: 0.5 mg ml-1; temperature: 25ºC; contact time: 90 min; adsorbent dosage: 20 mg, c) Initial LYS concentration to the adsorbing process (pH: 6.2; temperature: 25ºC; contact time: 90 min; adsorbent dosage: 20 mg. d) Adsorbent dosage to the adsorbing process (pH: 6.2; temperature: 25ºC; initial LYS concentration: 0.5 mg ml-1 contact time: 90 min), e) Ionic strength to the adsorbing process (pH: 6.2; temperature: 25ºC; initial LYS concentration: 0.5 mg ml^{-1}; contact time: 90 min; adsorbent dosage: 15 mg).

contact time resulted in slow improvement [19]. In fact, remarkable adsorption capacity was achieved during the first 30 min of the reaction. According to the figure, it seems that equilibrium between LYZ and Fe_3O_4@IG reached within 160 min. Generally, at the initial stage of the adsorption process, there are numerous vacant sites on the adsorbent surface which easily can be accessed by LYZ molecules in which engender rapid adsorption. On the other hand, once sites are merely occupied by the pollutant molecules, attraction energy of adsorbent will reduce and due to the repulsive force between bulk solution and LYZ molecules, adsorption rate decreases greatly. On the basis of the time saving and adsorption capacity, the authors decided to fix contact time to be 90 min for further experiments.

The effect of pH

Various studies have pointed out that the initial pH of the solution is a key parameter that highly affects the degree of pollutant ionization as well as a surface charge of the adsorbent. Indeed, the pH impacts the LYZ removal efficiency considerably. LYZ, like any other enzyme, is not active in a vast range of pH and former studies revealed that LYZ is active in the pH range of 6 to 10. The effect of pH on removal efficiency is shown in Figure 4b at contact time and adsorbent dosage of 90 min and 20 mg, respectively. It shows that by increasing the pH value from 6.2 to 8, adsorption capacity decreased rapidly from 95.25 to 79.25 mg/g. Thus, an optimum pH value of 6.2 was chosen for further experiments. Higher removal efficiency was achieved in acidic media. The main reason for such a behavior can be attributed to the electrostatic repulsion force between LYZ and Fe_3O_4@IG. Previous studies have pointed that the isoelectric of LYZ is 11.2 and it is positively charged under the pH value of 11 so for a good adsorption process, adsorbent must have owns negative charges. In the solution, there are plenty of phosphate ions that tend to interact with positive surface charges of Fe_3O_4@IG (NH_4^+ ions) that leads to observe an adsorbent with a negative charge that now is able to interact with the positive-charged protein. In fact, electrostatic repulsion force between

adsorbent and adsorbate is significantly reduced by phosphate ions. Fortunately, by reducing the pH value, LYZ takes more and more positive charges that induce more adsorption capacity and therefore higher removal efficiency. Based on these facts, optimum pH value was fixed at 6.2 for the following experiments.

The effect of initial LYZ concentration

The effect of initial LYZ concentration was investigated with various initial concentrations in the range of 0 to 1.2 mg/ml under optimum conditions (contact time 90 min, pH 6.2) and the results were presented in Figure 4c. The adsorbent dosage was fixed at 20 mg. As shown in the figure, by increasing the LYZ concentration from 0 to 0.7 mg ml^{-1}, adsorption capacity rapidly increased from 0 to 124.5 mg g^{-1}. There is an interesting point that when LYZ concentration is somehow beyond 0.7 mg ml^{-1}, adsorption capacity did not alter significantly. It should be noted that adsorbent dosage is fixe so there is a specified number of sites that LYZ molecules are able to occupy. When the adsorbent sites are totally saturated by pollutant molecules, a further increase in LYZ concentration has no effect on the adsorption process. In fact, an excess amount of LYZ will remain in the solution without any purification. Thus, for an optimum design of an adsorption process, a balance between adsorbent dosage and LYZ concentration must be considered. Based on the obtained results, LYZ concentration was chosen to be 0.5 mg ml^{-1}.

Effect of adsorbent dosage

The amount of adsorbent employed during water or wastewater purification, directly influence the cost of the treatment method, so the determination of the adsorbent optimum value is of great importance. The effect of various adsorbent dosages on adsorption capacity is presented in Figure 4d. It can be observed that by increasing the adsorbent dosage from 10 mg to 25 mg, adsorption capacity decreased from 141.5 to 21.2 mg/g. A closer look at the figure reveals that little fluctuation in adsorbent capacity when the adsorbent dosage was increased from 10 mg to 15 mg. Once the adsorbent dosage is implied to be beyond 15 mg, adsorption capacity significantly decreased to a great extent. Adsorption is controlled by adsorbent pores. When a high amount of adsorbent is used, it can be seen that adsorbent particles collide with each other and a lager particle with less surface area will be generated which is not fully desired for adsorption mechanism. So, optimum adsorbent dosage was to be 15 mg for the further experiments.

Effect of ionic strength

Ionic strength is an important parameter that influences adsorption efficiency depending on the main adsorption mechanism. In this direction, the effect of NaCl concentration on the adsorption capacity of the Fe_3O_4@IG was studied. As shown in Figure 4e, the adsorption capacity of LYS on Fe_3O_4@IG was sharply declined as the ionic strength increased from 0% to 20% w/v NaCl. Salt addition can enhance the contact of inner hydrophobic areas of protein to solution due to the hydration effect of salt molecules around the protein. That means the hydrophobic interactions between proteins and adsorbents are increased in the presence of salts. In contrast, the introduction of salt can lead to reduced electrostatic interaction between adsorbents and adsorbate. Therefore, depending on the main mechanism for protein adsorption (electrostatic or hydrophobic interaction) the adsorption efficiency of protein could be decreased or increased in the presence of salt. The experimental results confirmed that the electrostatic interaction is the main force for the adsorption of LYZ on Fe_3O_4@IG. Since electrostatic attractive interaction is the main driving force for the adsorption of LYZ by Fe_3O_4@IG, a high concentration of sodium ions can compete with positively charged LYZ and preferentially interact with negatively charged Fe_3O_4@IG, thus leading to the reduction of the adsorbed amount of LYZ (Figure 4).

Repeatability

There is no any doubt that an important factor for the suitability of a synthesized adsorbent to be used in industrial scale is the capability of the adsorbent to be regenerated and reused with approximately high performance as the first usage. From an economical point of view, that is so considerable. In the present study, the reusability of Fe_3O_4@IG for LYZ adsorption was examined for 3 cycles under optimum conditions. The results are listed in Table 1. As a result, Fe_3O_4@IG exhibited a great performance where adsorption capacity decreased only from 136.4 to 142.3 mg g^{-1} after 3 times repeated use. Furthermore, the Relative Standard Deviation (RSD) was calculated roughly 3.23% and it was acceptable. It can be concluded that synthesized Fe_3O_4@IG adsorbent is not only an efficient adsorbent but also owns great potential for reusability.

Desorption of lysozyme from Fe_3O_4@IG

As fully described in section 2.6 the desorption efficiency was investigated in the absence and the presence of the NaCl. To describe the obtained date, in the absence of NaCl the desorption efficiency was less than 30.6%, however, in the presence of the NaCl 10% w/v, the desorption efficiency was 85.5%. The reason for these phenomena are due to the fact that when there is no NaCl in the solution, the main driving force for the adsorption is electrostatic attraction, while by adding NaCl to the solution the adsorption force is based on the ion exchange mechanism and therefore sodium ions can compete with LYZ and replace positively charged LYZ from Fe_3O_4@IG.

Adsorption isotherms

Adsorption isotherms are an inevitable part of adsorption studies which state that in an equilibrium state, there is a relationship between the amount of solutes remain in the solution and the amount of the solute adsorbed on the adsorbent surface under fixed temperature conditions. In other words, adsorption isotherms give a better understanding of the adsorption mechanism. In the present study, two mostly used isotherms, Langmuir and Freundlich, were examined. Langmuir and Freundlich isotherm models are applicable to liquid-solid adsorption systems. Langmuir isotherm is one of the earliest models that used to describe adsorption over monolayer coverage of adsorbate and a finite number of active sites on the adsorbent surface. Freundlich isotherm assumes that the adsorbent surface is heterogeneous and monolayer or multilayer coverage of adsorbate can be observed. The Freundlich and Langmuir linear model can be expressed as Equation (1) and (2), respectively [20,21].

$$Lnq_e = LnK_F + \frac{1}{n}LnC_e \quad (1)$$

$$\frac{1}{q_e} = \frac{1}{q_m} + \frac{1}{K_L q_m C_e} \quad (2)$$

where K_F (mg g^{-1}) and 1/n are the Freundlich characteristic constants, reflecting the adsorption capacity and the adsorption intensity, respectively, K_L (ml mg^{-1}) is related to the energy of adsorption, q_e (mg g^{-1}) is the amount of lysozyme adsorbed at equilibrium time, q_m (mg g^{-1}) is the maximum adsorption amount of lysozyme, and C_e (mg ml^{-1}) is the equilibrium concentration of lysozyme in solution.

Non linear isotherm curves of Freundlich and Langmuir equation are shown in Figure 5a and 5b, respectively. The favorability of the

Table 1: Repeatability of the Fe_3O_4@IG for LYS.

Run	qe (mg.g^{-1})	RSD (%)
1	136.4	
2	133.6	3.23
3	142.3	

adsorption process was determined by Freundlich constant n. In this study, n value was found to be 1.07 which is less than 10 and it shows that the adsorption of LYZ onto Fe_3O_4@IG was favorable in terms of adsorption mechanism. The best isotherm was chosen on the basis of the minimal deviation from the integral equation. The obtained results showed that the correlation coefficient (R^2) value for Langmuir isotherm (0.9533) is much greater than Freundlich isotherm (0.8366). Furthermore, the maximum adsorption capacity of LYZ onto the Fe_3O_4@IG calculated from Langmuir isotherm was found to be 149.25 mg g^{-1} which was in accordance with the maximum adsorption capacity found during experimental data and under optimum conditions (136.9 mg g^{-1}). These results reflected that the adsorption process of LYZ followed Langmuir isotherm model and monolayer coverage of LYZ on the surface of the Fe_3O_4@IG can be predicted.

In terms of LYZ adsorption with various adsorbents, Table 2 was prepared based on the adsorbent used and maximum adsorption capacity. According to Table 2, the adsorption capacity of the synthesized Fe_3O_4@IG adsorbent is higher than other adsorbents except for one study that used agarose based beads as an adsorbent. It is fairly to conclude that synthesized adsorbent in this study has a better performance during the adsorption process for water and wastewater purification (Figure 5, Table 2).

Adsorption kinetics

Like any other chemical reactions or physical phenomena, determination of the reaction speed is of great importance. Adsorption kinetics mainly discusses the time required to adsorbed solute from bulk solution into the adsorbent surface. In the present study, adsorption kinetics namely, Pseudo First Order (PFO) and Pseudo Second Order (PSO) models were utilized to explain the LYZ adsorption process. PFO was firstly proposed by Lagergren which assumes that the adsorption rate is proportional to the difference between equilibrium adsorption capacity and adsorption capacity and the amount of solute adsorbed at determine time [22]. PSO model is based on the fact that the adsorption rate does not follow a linear equation between adsorption capacity and the amounts of solute adsorbed at determine time. The PFO and PSO models can be expressed as Equations (3) and (4), respectively [23,24].

$$\frac{1}{q_t}=\frac{K_1}{q_e t}+\frac{1}{q_e} \quad (3)$$

$$\frac{t}{q_t}=\frac{1}{k_2 q_e^{\,2}}+\frac{t}{q_e} \quad (4)$$

where k_1 (min^{-1}) and k_2 (g mg^{-1}.min^{-1}) are the pseudo-first-order rate constant and pseudo-second-order rate constant, respectively, q_t (mg^{-1}) and q_e (mg.g^{-1}) are the adsorbed amounts of LYZ at any and equilibrium time (min), respectively.

Figure 6a and 6b shows PFO and PSO curves respectively. The higher R^2 value obtained from PSO suggested that the experimental data are better fitted to PSO than PFO. To confirm the obtained results, the calculated adsorption capacity of PFO and PSO were calculated [25,26]. It was found that adsorption capacity related to experimental data and the calculation methods were close to each other for the PSO model. These results suggested that the experimental kinetic data for LYZ adsorption onto Fe_3O_4@IG complied PSO model. It should be noted that chemisorption is the dominant interaction between LYZ molecules and Fe_3O_4@IG in which they both tend to share their electron with each other [27-30]. The obtained results can be confirmed by the FTIR test that proved the presence of the functional groups on the surface of the adsorbent [30] (Figure 6).

Separation of LYZ from protein mixture and egg white solutions

As shown in Figure 7, the LYZ was selectively separated from the binary protein mixture, only LYZ could be found in sample 5 of Figure 7, therefore the purity of LYZ was very high [31-33]. The SDS-PAGE of the source chicken egg white solution, the supernatant after adsorption and the eluted solution is shown in Figure 7. The SDS-PAGE electropherogram clearly shows that only LYZ was detected in the band of the eluted solution (sample 6 in Figure 7). Therefore, the separated lysozyme has high purity [34,35].

Conclusion

In this study, Fe_3O_4@IG was used as an efficient magnetic adsorption for separation of lysozyme from aqueous solutions. The results showed that under the optimum condition the synthesized adsorbent has a high capacity for lysozyme. The effect of ionic

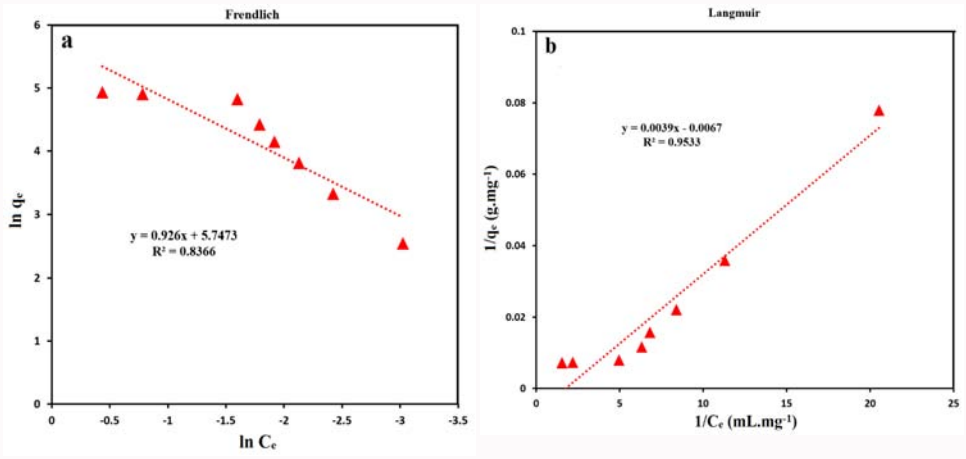

Figure 5: a) Freundlich, b) Langmuir adsorption isotherm of lysozyme by Fe_3O_4@IG.

Table 2: Maximum adsorption capacity of lysozyme on various adsorbents.

Adsorbents	Maximum adsorption capacity (mg.g-1)	References
Reactive Red 120 modified magnetic chitosan microspheres	144.9	[25]
Lysozyme specific aptamer immobilized MCM-41 silicate	36.8	[26]
Sulfonated poly(glycidyl methacrylate) grafted cellulose	141.67	[27]
Tris(hydroxymethyl)amino methane-modified magnetic microspheres	108.6	[28]
Chitin-silica-based affinity chromatographic matrix	117.1	[29]
Acrylic acid copolymer based beads (Hydrolite D115)	48.9	[30]
Agarose based beads (CM Sepharose 6 Fast Flow)	165.8	[30]
Monolithic molecularly imprinted cryogel	36.3	[31]
Hybrid Zwitterionomer	130	[32]
PAA-modified Fe_3O_4@silica core/shell microspheres	127	[33]
Fe_3O_4@SiO_2@IL	20	[34]
Carbon-Coated Fe_3O_4 Nanoparticles	76.34	[35]
Fe_3O_4@IG	149.25	Present study

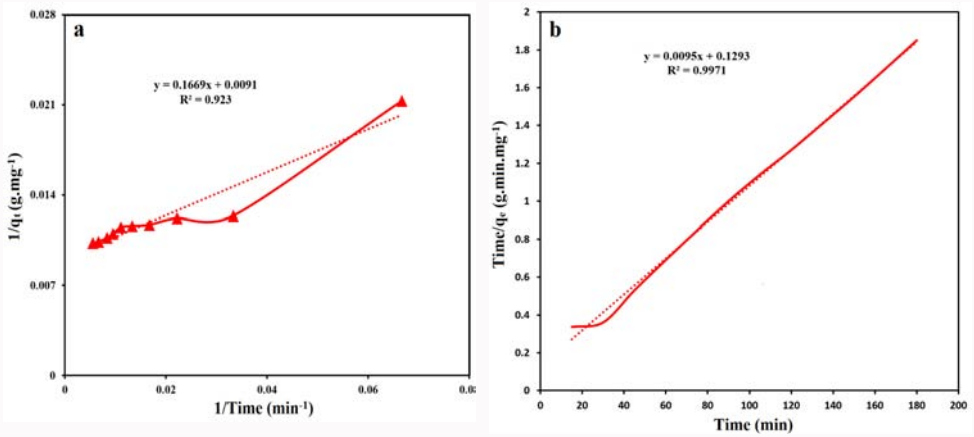

Figure 6: a) Pseudo-first-order and (b) Pseudo-second-order kinetics curves.

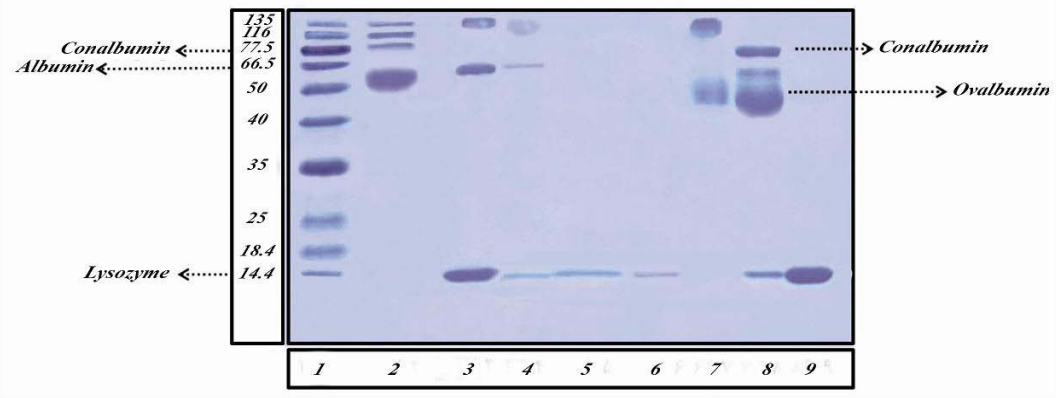

Figure 7: SDS Gel electrophoresis of lysozyme adsorption experiment from protein mixture and whole egg white. The Sample are 1) protein standard markers, 2) commercial BSA, 3) the stock binary protein solution, 4) the remaining protein solution after magnetic separation, 5) eluted lysozyme from the Fe_3O_4@Isinglass after adsorption in mixture, 6) eluted lysozyme from the Fe_3O_4@Isinglass after adsorption in egg white solution, 7) the remaining egg white after treatment with the Fe_3O_4@Isinglass, 8) total whole egg white before adsorption, and 9) commercial lysozyme.

strength on the adsorption process revealed that the dominant mechanism in the adsorption is based on the electrostatic attraction, so for lysozyme desorption, a salt addition was conducted, and 85.5% of lysozyme was separated from the adsorbent. Additionally, the RSD value of the process was 3.2% after three times which was acceptable.

PSO and Langmuir were best models to describe adsorption rate and adsorption isotherm, respectively. Fe_3O_4@IG demonstrated highly effective and selective adsorption of LYZ from chicken egg white. Thus, Fe_3O_4@IG can be nominated as a suitable adsorbent to separate LYZ from different media with high adsorption capacity.

Acknowledgment

The authors wish to express their gratitude for the financial support provided by the Research Council of Iran University of Science and Technology (IUST), Tehran, Iran.

References

1. Wu T, Jiang Q, Wu D, Hu Y, Chen S, Ding T, et al. What is new in lysozyme research and its application in food industry? A review. Food Chem. 2019;274:698-709.
2. Wu T, Huang J, Jiang Y, Hu Y, Ye X, Liu D, et al. Formation of hydrogels based on chitosan/alginate for the delivery of lysozyme and their antibacterial activity. Food Chem. 2018;240:361-9.
3. Leśnierowski G, Cegielska-Radziejewska R, Kijowski J. Antibacterial activity of thermally modified lysozyme. Food Sci Technol. 2001;4(2):17.
4. Dembczynski R, Bialas W, Regulski K, Jankowski T. Lysozyme extraction from hen egg white in an aqueous two-phase system composed of ethylene oxide–propylene oxide thermo separating copolymer and potassium phosphate. Process Biochem. 2010;45(3):369-74.
5. Hartono YD, Lee AN, Lee-Huang S, Zhang D. Computational study of bindings of HL9, a nonapeptide fragment of human lysozyme, to HIV-1 fusion protein gp41. Bioorg Med Chem Lett. 2011;21(6):1607-11.
6. Ye J, Wang C, Chen X, Guo S, Sun M. Marine lysozyme from a marine bacterium that inhibits angiogenesis and tumor growth. Appl Microbiol Biotechnol. 2008;77(6):1261-7.
7. Casini A, Mastrobuoni G, Temperini C, Gabbiani C, Francese S, Moneti G, et al. ESI mass spectrometry and X-ray diffraction studies of adducts between anticancer platinum drugs and hen egg white lysozyme. Chem Commun (Camb). 2007;(2):156-8.
8. Wan Y, Lu J, Cui Z. Separation of lysozyme from chicken egg white using ultra filtration. Sep Purif Technol. 2006;48(2):133-42.
9. Chang HM, Yang CC, Chang YC. Rapid separation of lysozyme from chicken egg white by reductants and thermal treatment. J Agric Food Chem. 2000;48(2):161-4.
10. Noh KH, Imm JY. One-step separation of lysozyme by reverse micelles formed by the cationic surfactant, cetyl di methyl ammonium bromide. Food Chem. 2005;93(1):95-101.
11. Roy I, Rao MVS, Gupta MN. Purification of lysozyme from other hen's-egg-white proteins using metal-affinity precipitation. Biotechnol Appl Biochem. 2003;37(1):9-14.
12. Cohen JL, Barile D, Liu Y, de Moura Bell JMLN. Role of pH in the recovery of bovine milk oligosaccharides from colostrum whey permeate by nanofiltration. Int Dairy J. 2017;66:68-75.
13. Durance TD. Separation, purification, and thermal stability of lysozyme and avidin from chicken egg white. Egg Uses and Processing Technologies: New Developments. Wallingford, UK: CAB International Press. 1994;77-93.
14. Tong XD, Sun Y. Nd-Fe-B alloy-densified agarose gel for expanded bed adsorption of proteins. J Chromatogr A. 2002;943(1):63-75.
15. Thakur S, Pandey S, Arotiba OA. Sol-gel derived xanthan gum/silica nano composite-a highly efficient cationic dyes adsorbent in aqueous system. Int J Biol Macromol. 2017;103:596-604.
16. Hickman D, Sims TJ, Miles CA, Bailey AJ, de Mari M, Koopmans M. Isinglass/collagen: Denaturation and functionality. J Biotechnol. 2000;79(3):245-57.
17. Weber P, Steinhart H, Paschke A. Characterization, antigenicity and detection of fish gelatine and isinglass used as processing aids in wines. Food Addit Contam Part-A Chem Anal Control Expo Risk Assess. 2010;27(3):273-82.
18. Beveridge JMR, Lucas CC. Amino acids of isinglass. J Biol Chem. 1944;155:547-56.
19. Ghenaatgar A, Tehrani R, Khadir A. Photocatalytic degradation and mineralization of dexamethasone using WO_3 and ZrO_2 nanoparticles: Optimization of operational parameters and kinetic studies. J Water Process Eng. 2019;32.
20. Mohammadi A, Khadir A, Tehrani RMA. Optimization of nitrogen removal from an anaerobic digester effluent by electro coagulation process. J Environ Chem Eng. 2019;7(3).
21. Piri F, Mollahosseini A, khadir A, Milani Hosseini M. Enhanced adsorption of dyes on microwave-assisted synthesized magnetic zeolite-hydroxyapatite nanocomposite. J Environ Chem Eng. 2019;7(5):103338.
22. Beheshti F, Tehrani RMA, Khadir A. Sulfamethoxazole removal by photo catalytic degradation utilizing TiO_2 and WO_3 nanoparticles as catalysts: Analysis of various operational parameters. Int J Environ Sci Technol. 2019;16(12):7987-96.
23. Mirjavadi ES, Tehrani RMA, Khadir A. Effective adsorption of zinc on magnetic nano composite of Fe_3O_4/zeolite/cellulose nanofibers: kinetic, equilibrium, and thermodynamic study. Environ Sci Pollut Res Int. 2019;26(32):33478-93.
24. Mollahosseini A, Khadir A, Saeidian J. Core–shell polypyrrole/Fe_3O_4 nano composite as sorbent for magnetic dispersive solid-phase extraction of Al+3 ions from solutions: investigation of the operational parameters. J Water Process Eng. 2019;29:100795.
25. Li Z, Cao M, Zhang W, Liu L, Wang J, Ge W, et al. Affinity adsorption of lysozyme with Reactive Red 120 modified magnetic chitosan microspheres. Food Chem. 2014;145:749-55.
26. Bayramoglu G, Ozalp VC, Yilmaz M, Guler U, Salih B, Arica MY. Lysozyme specific aptamer immobilized MCM-41 silicate for single-step purification and Quartz Crystal Microbalance (QCM)-based determination of lysozyme from chicken egg white. Microporous Mesoporous Mater. 2015;207:95-104.
27. Anirudhan TS, Senan P. Adsorptive potential of sulfonated poly (glycidylmethacrylate)-grafted cellulose for separation of lysozyme from aqueous phase: Mass transfer analysis, kinetic and equilibrium profiles. Colloids Surfaces A Physicochem Eng Asp. 2011;377:156-66.
28. Zhang G, Cao Q, Li N, Li K, Liu F. Tris (hydroxymethyl) amino methane-modified magnetic microspheres for rapid affinity purification of lysozyme. Talanta. 2011;83(5):1515-20.
29. Wolman FJ, Copello GJ, Mebert AM, Targovnik AM, Miranda MV, NAvarro del Canizo AA, et al. Egg white lysozyme purification with a chitin–silica-based affinity chromatographic matrix. Eur Food Res Technol. 2010;231(2):181-8.
30. Cheng YM, Jin XH, Gao D, Xia HF, Chen JH. Thermodynamics and kinetics of lysozyme adsorption onto two kinds of weak cation exchangers. Biotechnol Bioprocess Eng. 2013;18(5):950-5.
31. Rabieizadeh M, Kashefimofrad SM, Naeimpoor F. Monolithic molecularly imprinted cryogel for lysozyme recognition. J Sep Sci. 2014;37(20):2983-90.
32. Chakrabarty T, Kumar M, Shahi VK. pH responsive hybrid zwitterionomer for protein separation: Smart nanostructured adsorbent. Ind Eng Chem Res. 2012;51(7):3015-22.
33. Shao D, Xu K, Song X, Hu J, Yang W, Wang C. Effective adsorption and separation of lysozyme with PAA-modified Fe_3O_4@silica core/shell microspheres. J Colloid Interface Sci. 2009;336(2):526-32.
34. Wei Y, Li Y, Tian A, Fan Y, Wang X. Ionic liquid modified magnetic microspheres for isolation of heme protein with high binding capacity. J Mater Chem B. 2013;1:2066-71.
35. Wang L, Kim C, Zhang Z, Hu Q, Sun T, Hu X. Adsorption behavior of lysozyme on carbon-coated Fe_3O_4 nanoparticles. Curr Nanosci. 2017;13(2):159-66.